Science of the Total Environment 807 (2022) 150878

Contents lists available at ScienceDirect

Science of the Total Environment

journal homepage: www.elsevier.com/locate/scitotenv

Dynamics of microbial community and their effects on membrane fouling in an anoxic-oxic gravity-driven membrane bioreactor under varying solid retention time: A pilot-scale study

Anjan Deb [a,b,*], Khum Gurung [a], Jannatul Rumky [a], Mika Sillanpää [c,d,e,f,g,h], Mika Mänttäri [a], Mari Kallioinen [a]

[a] Department of Separation Science, School of Engineering Science, Lappeenranta-Lahti University of Technology (LUT University), Sammonkatu 12, 50130 Mikkeli, Finland
[b] Department of Chemistry, University of Helsinki, P.O. Box 55 (A.I. Virtasen aukio 1), 00014 Helsinki, Finland
[c] Department of Chemical Engineering, School of Mining, Metallurgy and Chemical Engineering, University of Johannesburg, P. O. Box 17011, Doornfontein 2028, South Africa
[d] School of Chemical and Metallurgical Engineering, University of the Witwatersrand, 2050 Johannesburg, South Africa
[e] Chemistry Department, College of Science, King Saud University, Riyadh 11451, Saudi Arabia
[f] School of Resources and Environment, University of Electronic Science and Technology of China (UESTC), NO. 2006, Xiyuan Ave., West High-Tech Zone, Chengdu, Sichuan 611731, PR China
[g] Faculty of Science and Technology, School of Applied Physics, University Kebangsaan Malaysia, 43600 Bangi, Selangor, Malaysia
[h] School of Chemistry, Shoolini University, Solan, Himachal Pradesh 173229, India

HIGHLIGHTS

- GD-MBR operation with real municipal wastewater was evaluated at different SRTs.
- SRT had significant influence on microbial community and membrane fouling.
- Abundance of quorum quenching bacterial genera were obtained at SRT of 25 days.
- Carbohydrate content of SMP and TB-EPS showed positive correlation with the floc size.
- SRT of 25 days permitted the longest operating time with minimum membrane fouling rate.

GRAPHICAL ABSTRACT

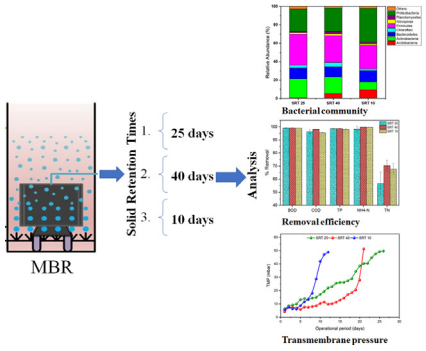

ARTICLE INFO

Article history:
Received 29 July 2021
Received in revised form 24 September 2021
Accepted 4 October 2021
Available online 8 October 2021

Editor: Paola Verlicchi

Keywords:
Membrane bioreactor
Membrane fouling
Solid retention time
Floc size distribution
Microbial community dynamics

ABSTRACT

Membrane fouling in a membrane bioreactor (MBR) is highly influenced by the characteristics of the influent, the mixed liquor microbial community and the operational parameters, all of which are environment specific. Therefore, we studied the dynamics of microbial community during the treatment of real municipal wastewater in a pilotscale anoxic-oxic (A/O) MBR equipped with a gravity-driven membrane filtration system. The MBR was operated at three different solid retention times (SRTs): 25, 40 and 10 days for a total period of 180 days in Nordic environmental conditions. Analysis of microbial community dynamics revealed a high diversity of microbial species at SRT of 40 days, whereas SRT of 25 days was superior with microbial richness. Production of soluble microbial products (SMP) and extracellular polymeric substances (EPS) was found to be intensely connected with the SRT and food to microorganism (F/M) ratio. Relatively longer operational period with the lowest rate of membrane fouling was observed at SRT of 25 days, which was resulted from the superior microbial community, lowest production of SMP and loosely bound EPS as well as the lower filtration resistance of larger sludge flocs. Abundance of quorum quenching (QQ) bacteria and granular floc forming bacterial genera at SRT of 25 days provided relatively lower membrane fouling tendency and larger floc formation, respectively. On the other hand, substantial amount of various surface colonizing and EPS producing bacteria was found at SRT of 10 days, which

* Corresponding author at: Department of Chemistry, University of Helsinki, P.O. Box 55 (A.I. Virtasen aukio 1), 00014 Helsinki, Finland.
E-mail address: anjan.deb@helsinki.fi (A. Deb).

https://doi.org/10.1016/j.scitotenv.2021.150878

promoted more rapid membrane fouling compared with the fouling rate seen at other tested SRTs. To sum up, this research provides a realistic insight into the impact of SRT on microbial community dynamics and resulting characteristics of mixed liquor, floc size distribution and membrane fouling for improved MBR operation.

1. Introduction

The rising concern of water pollution and the demand for water reuse are imposing strict discharge standards to the wastewater treatment plants. As a result, membrane bioreactor (MBR), due to its ability to meet up the rigid effluent standards with a limited reactor volume and waste generation, has received considerable acceptance for the treatment and reclamation of both municipal and industrial wastewater (Gurung et al., 2019, 2017; Yurtsever et al., 2021). The MBR process combines the biological activated sludge process with membrane filtration, which offers several benefits over the conventional activated sludge process, including smaller plant footprint, enhanced removal of organic pollutants, complete retention of suspended solids and lower sludge production (Gurung et al., 2019; Krzeminski et al., 2017; Meng et al., 2017). However, the costs associated with the operation and membrane-fouling control remains as the major constraints of MBRs application (Deng et al., 2015; Meng et al., 2017, 2008).

Higher operating expenses in MBR operations are associated with the high energy consumption required to maintain adequate transmembrane pressure (TMP) for improved productivity and the delivery of scouring air to minimize membrane fouling. The energy required to maintain a high TMP can be reduced significantly using gravity-driven (GD) membrane filtration technology, which enables the process to run at low TMP with biofilm-controlled flux stabilization (Fortunato et al., 2020; Pronk et al., 2019). Membrane fouling, on the other hand, remains to be the most problematic aspects of GD-MBR operation to deal with. Membrane fouling occurs as a result of complex interaction between the activated sludge and membrane surface properties and poses several challenges including membrane pore blocking, permeate flux decline and the need for chemical cleaning of membrane during MBRs operation (Gao et al., 2010; Long et al., 2021; Meng et al., 2017; Wu et al., 2020). Recently, Fortunato et al. studied the membrane fouling control in a GD-MBR using different physical cleaning strategies such as membrane relaxation and air scouring. The addition of air scouring after a relaxation cycle resulted in a significant increase in biomass removal from the membrane surface, as well as increase in performance (Fortunato et al., 2020). While using a specific membrane, the operational conditions and microbial populations in the mixed liquor have the substantial impact on membrane fouling in MBRs.

Solid retention time (SRT) or mean cell residence time is considered as one of the key operational parameters that significantly affects the activated sludge characteristics in terms of microbial diversity, biodegradation kinetics, biopolymer concentration, floc formation and size distribution, which in turn affects the effluent quality and membrane-fouling tendency (Ahmed et al., 2007; Han et al., 2005; Meng et al., 2017; Yu et al., 2018). For example, MBR operation at short SRT (e.g. 10 days) limits the growth of functional micro-organisms such as slow-growing nitrifiers (Yu et al., 2018). On the other hand, process operation at longer SRT allows the extensive growth of biomass concentration, which results in substrate deficiency, mass transfer limitations, enhanced aeration cost and membrane fouling (Laera et al., 2007). As a result, immense efforts have been made by the researchers over the last decades to establish a reliable relationship between the SRT, biomass characteristics and membrane fouling (Duan et al., 2014; Han et al., 2005; Lee et al., 2003; Ouyang and Liu, 2009; Yu et al., 2018). However, experimental outcomes are often contradictory when they shift from lab scale to pilot scale and from synthetic wastewater to real wastewater. Therefore, more experimental evidence is required to improve the understanding of SRT effects on biomass characteristics and membrane fouling.

Microbial communities and their dynamics in the activated sludge play a crucial role in the degradation of various organic and inorganic pollutants as well as in the development of microbial colonization on the membrane surface, which further promotes the membrane fouling (ElNaker et al., 2018; Takimoto et al., 2021). Besides that, various microbial activities in the bioreactor, such as microbial growth, secretion and substrate consumption stimulates the production of soluble microbial products (SMP) and extracellular polymeric substances (EPS) (Li et al., 2008; Lin et al., 2014). Various experimental studies revealed that EPS comprises a complex mixture of high molecular weight bio-polymeric substances such as carbohydrate, proteins, humic substances and nucleic acids (Frølund et al., 1996; Lin et al., 2014). As a result, EPS creates a highly hydrated gel-like three-dimensional matrix around the microbial aggregates and prevents the cells from the adverse environmental effects (Shi et al., 2017). Moreover, significant contribution of EPS on floc formation and size distribution as well as membrane fouling in MBRs has been evident in many previous researches (Li and Yang, 2007; Teng et al., 2019; Wang et al., 2009). However, the experimental outcomes concerning the effects of SRT on the growth and diversity of the microbial community, biopolymer production and their composition, role of SMP and EPS in floc formation and floc size distribution at various environmental conditions are often contradictory (Ouyang and Liu, 2009; Van den Broeck et al., 2012; Wang et al., 2014) and have not been well reported. Therefore, an in-depth understanding of the influences of operating conditions in pilot-scale MBR, particularly the SRT, can forward the better process exploitation and optimization.

In this study, we aimed to investigate the effect of three different SRTs (10, 25 and 40 days) on the performance of a pilot-scale gravity-driven A/O MBR system treating real municipal wastewater. We evaluated the sludge microbial community dynamics and their contribution in pollutant degradation, biopolymer (dissolved and bound EPS) production and their composition, floc size distribution, treated effluent quality and membrane fouling in the MBR process at varying SRTs. The dynamics of microbial community in the mixed liquor at different SRTs were analyzed using the next-generation sequencing methods. Furthermore, fouling development on the membrane surface was observed by monitoring the rate of TMP rise during the process operation.

2. Materials and methods

2.1. Description of MBR pilot plant

The pilot-scale MBR plant (Aquazone Oy, Finland) used in this study comprised of a screening tank, pre-clarifier, anoxic tank, aeration tank, membrane tank and deoxygenation tank (Fig. 1). It was installed and operated at Kenkäveronniemi Wastewater Treatment Plant in Mikkeli, Finland. The total biological volume of the plant was 28 m^3, including major compartments of cylindrical shaped aeration and membrane tank (10 m^3 each), rectangular-shaped anoxic tank (6.0 m^3) and a deoxygenation tank (2.0 m^3). The flat sheet microfiltration membrane modules of 0.2 μm PVDF membrane (Alfa Laval MFM100, Sweden) with a total surface area of 154 m^2 were employed for filtration. The membrane module was completely submerged in the MBR tank, which had a water level above the permeate extraction line. The water column at the module's head generates sufficient TMP to force the permeate through the membrane. When all permeate line valves are open,

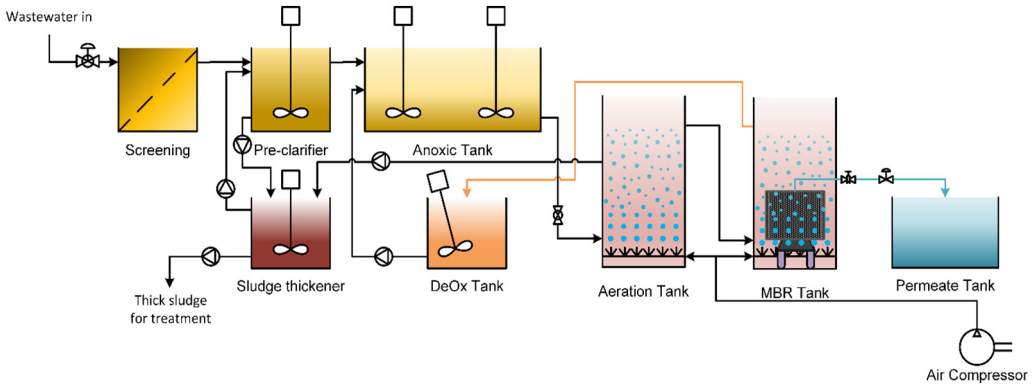

Fig. 1. MBR pilot plant used in the experiments.

permeate flows by gravity from the MBR to the permeate tank and the permeate flux was regulated using a flow control valve. The membrane module was equipped with an S-shaped aeration system for membrane air scouring and maintaining aerobic biological ambiance inside the system.

2.2. Operation of MBR

The MBR was operated continuously after the initial inoculation and acclimatization of activated sludge for a month. Process parameters, such as wastewater flowrate, pH, and temperature were continuously monitored online. Municipal wastewater, after a preliminary coarse screening followed by a fine screening (2 mm), was continuously fed to the primary clarifier. After the primary clarification, wastewater was fed to the anoxic tank, having the hydraulic retention time (HRT) of around 3 h. Then, the wastewater entered the aeration tank and finally to the membrane tank for initiating nitrification and other biological degradation processes. The HRT in the aeration tank was about 5 h and the dissolved oxygen concentration was maintained around 2 mg/l. The rejected mixed liquor was recycled from the MBR to the anoxic zone after deoxygenation with a recycling rate of 4.5 m^3/h.

During the process operation, SRT was maintained by discarding the calculated amount of activated sludge from the aeration tank on an hourly basis at an intermittent mode. The amount of sludge discarded during SRT of 25, 40 and 10 days was 1.1, 0.7 and 2.8 m^3/day, respectively. At each SRT, there was an adaptation period followed by a stabilized period. The adaptation period was maintained at least equal to the number of operational days for SRT of 25 and 10 days, while SRT of 40 days was maintained a little differently. After the completion of SRT 25 stabilized period, the process was operated for another 15 days without removing any sludge from the process so that the final SRT reached the sludge age of approximately 40 days. The system was then continuously adapted at SRT of 40 days by discarding sludge at a rate of 0.7 m^3/day from the process for another 14 days prior to the start of the stabilization and sampling period.

In the membrane tank, an intermittent filtration of 10 min followed by 2 min relaxation was maintained with an automatic flow control valve and the permeate was extracted through membranes by the virtue of gravitational pressure difference between water level of the membrane tank and permeate line (Fig. 1). Transmembrane Pressure (TMP) was recorded online using a pressure transmitter located in the permeate line. Air scouring was maintained continuously at a specific aeration demand of 0.45 $m^3/m^2 \cdot h$ to limit the reversible fouling effects during the operation. In-situ membrane cleaning was performed by using sodium hypochlorite solution followed by citric acid solution after each of the adaptation periods to ensure cleaned membrane surface during the actual sampling periods.

2.3. Analysis of microbial community

For the analysis of microbial community, activated sludge samples were collected weekly in a sterile container during the stabilized period from the MBR tank. After collection, 15 ml of sample was dispensed into a sterile Eppendorf tubes and centrifuged at 4000*g* at 4 °C for 15 min to decant the supernatant. The obtained sludge pellets were stored at −20 °C prior to DNA extraction.

Genomic DNA was extracted from sludge samples with DNeasy Powersoil kit (Qiagen Inc.) according to protocol provided by the manufacturer. About 500 mg (wet weight) of sludge sample was used for each extraction. Portion of bacterial 16S small ribosomal unit gene was amplified with primers 519F (5′-CAGCMGCCCGCGGTAATWC-3′) and 926R (5′-CCGTCAATTCCTTTRAGTTT-3′). Polymerase chain reactions (PCRs) were performed in 20 μl volume in three replicates, each containing 1× Phusion Flash High-Fidelity Master Mix (ThermoFisher Scientific, USA), 0.5 μM forward and reverse primers and 40 ng template DNA. After an initial 3-min denaturation at 98 °C, the following cycling conditions were used: 20 cycles of 98 °C, 10 s; 64 °C, 10 s; 72 °C, 30 s. Final extension step was carried out at 72 °C for 5 min.

After the amplification, triplicate reactions were pooled together and PCR products were purified using Ampure XP PCR cleaning kit (Agencourt Bioscience, USA) (Xie et al., 2021). Purity and concentration of PCR products were measured with a Bioanalyzer DNA-1000 chip. Equimolar amounts of each samples were pooled together, and pooled samples were further size-selected using Ampure XP kit. Prior to sequencing, final concentration of pooled samples was determined using Quant-iT PicoGreen dsDNA assay kit (ThermoFisher Scientific, USA).

Sequencing was performed on a two Ion 314 v2 chips using Ion Torrent PGM (Torrent Suite version 5.12.0) and Ion Torrent OT2 instruments, and Ion Hi-Q View OT2 and Ion Hi-Q View Sequencing kits (ThermoFisher Scientific, USA). Analysis of sequence data was carried out in QIIME 2 platform (version 2019.7.0) (Caporaso et al., 2010; Su et al., 2021). Before importing raw sequence data, cutadapt v.2.4 was used to remove reads shorter than 100 bp and raw reads were imported to QIIME 2 as multiplexed single-ended barcode included sequence data. Subsequently, reads were demultiplexed to samples based on barcode sequences and PCR primer sequences were trimmed from reads using QIIME 2 cutadapt plugin. Processed reads were denoised and dereplicated with truncation length of 300 bp using DADA2-pyro plugin (Callahan et al., 2016). Representative sequences of all unique amplicon sequence features were aligned with MAFFT (Katoh and Standley, 2013) and used to construct phylogenetic tree with FastTree2 (Price et al., 2010). Taxonomy was assigned to amplicon features using QIIME 2 feature-classifier (Bokulich et al., 2018) against the Greengenes 13_8 99% operational taxonomic unit (OTU) reference sequences (McDonald et al., 2012). Alpha diversity metrics were then estimated using QIIME 2 diversity plugin.

2.4. Analysis of water and activated sludge quality

Water quality indicators, such as total suspended solid (TSS), chemical oxygen demand (COD), biochemical oxygen demand (BOD), ammonium nitrogen (NH_4-N), total nitrogen (TN) and total phosphorous (TP), were analyzed from both influent and permeate samples using the standard procedure of wastewater analysis (Clesceri et al., 1998). The influent and permeate samples were collected weekly during the stabilized period. Mixed liquor suspended solids (MLSS), mixed liquor volatile suspended solids (MLVSS) and sludge volume index (SVI) were measured according to the protocol provided by American Public Health Association (APHA) (Clesceri et al., 1998). Besides, MLSS and Dissolved Oxygen (DO) concentration were continuously monitored and recorded online. Food to microorganism ratio (F/M) was calculated from the influent COD data using Eq. (1).

$$F/M = \frac{D_f \times COD}{C_{MLVSS} \times V_{bio}} \quad (1)$$

where D_f is the daily flowrate of feed wastewater entering into the process in m^3/day; COD is the chemical oxygen demand of the feed wastewater in mg/l; C_{MLVSS} is the concentration of MLVSS in g/l and V_{bio} is the volume of the total biological process in m^3.

2.5. Extraction and analysis of EPS

Different fractions of EPS, such as soluble EPS (also known as soluble microbial products or SMP) and bound EPS (B-EPS) were extracted from the mixed liquor samples according to the methodology reported by Y. Liu et al. (2018) and Rumky et al. (2018). Briefly, 40 ml of the mixed liquor samples were collected and subsequently centrifuged (4000*g*) at 4 °C, for 15 min. The supernatant was then filtered through 0.45 μm nylon membrane and collected as the SMP fraction for further analysis. The collected residual sludge pellets were then used for the B-EPS extraction into loosely bound EPS (LB-EPS) and tightly bound EPS (TB-EPS) fractions. The LB-EPS was extracted by re-suspending the sludge pellets in 40 ml of 0.5% NaCl solution. After the necessary vortex oscillation (1 min) and 5 min ultrasonication, the re-suspended pellets were centrifuged (4000*g*) for 15 min at 4 °C. The supernatant collected by filtering through a 0.45 μm nylon membrane was then further used for LB-EPS analysis. On the other hand, TB-EPS was extracted from the sludge pellets by re-suspending in 40 ml of 0.5% NaCl solution, followed by vortex oscillation (1 min), 5 min ultrasonication, 30 min thermal treatment at 70 °C and 15 min of centrifugation (4000*g*) at 4 °C. Finally, the supernatant collected by filtering through a 0.45 μm nylon membrane was used for the TB-EPS analysis.

Concentrations of EPS fractions (SMP, LB-EPS and TB-EPS) were measured as dissolved organic carbon (DOC) concentrations using Shimadzu TOC-V_{CPH} Analyzer. EPS fractions have also been characterized based on their protein and carbohydrate contents. Carbohydrate content of EPS fractions was measured by the Anthrone method, using glucose as the standard (Frølund et al., 1996). Furthermore, the Lowry method was used to determine the protein content in the EPS fractions using bovine serum albumin (BSA) as standard (Frølund et al., 1996; Raunkjær et al., 1994). The protein and carbohydrate contents of EPS fractions were analyzed using UV-spectrophotometer (PerkinElmer Lambda 45, USA) at maximum absorbances of 750 nm and 625 nm, respectively. All the measurements were triplicated.

2.6. Analysis of floc size distribution

The flocs size and their distributions in the activated sludge sample were carried out using a Mastersizer 2000 particle size analyzer (Malvern, UK). The formation of activated sludge flocs depends on the SRT and the biochemical composition of the sludge suspension. Therefore, the Pearson correlation analysis was performed using R statistical tool to understand the correlation between the SRT, activated sludge biochemical composition and d50 floc size.

3. Result and discussion

3.1. Effect of SRT on microbial community dynamics

3.1.1. Analysis of microbial community richness and diversity

Changing solid retention time in MBRs has been found to have notable effects on the microbial community (Yu et al., 2018). In this study, the Ion torrent sequencing method was applied to acquire information on the microbial community, their diversity and richness from the sludge samples collected at different SRTs. The adequacy of sequencing depth to reveal the diversity of bacterial communities at the examined SRTs can be interpreted from the rarefaction curves (Fig. 2a).

All the curves reached the plateau indicating the adequacy of sequencing depth in this study. The goodness of coverage for all the examined SRTs was 0.99, indicating that the Ion torrent sequencing was able to unveil most of the OTUs (Chen et al., 2017). The diversity and richness of the microbial communities in the samples were characterized by the Shannon diversity index and chao1 estimation, respectively (Fig. 2b). The Shannon diversity index accounts for both abundance and evenness of the microbial species available. The highest Shannon index (7.19) was observed at SRT 40 and the lowest (6.99) was at SRT 10. This result indicates that the microbial diversity increased with the increasing SRT. Likewise, Chao 1 indexes were estimated to be 825, 476 and 491 at SRT 25, 40 and 10 days, respectively. This result shows that the richness of microbial community was clearly highest when SRT was 25 days.

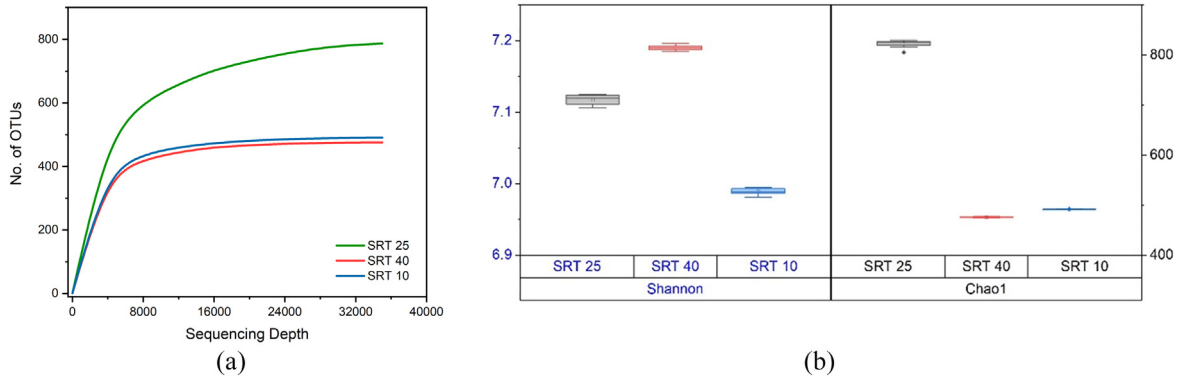

Fig. 2. (a) Rarefaction curves and (b) microbial richness and diversity analysis at different SRTs.

3.1.2. Phylogenetic analysis of microbial community

The phylogenetic analysis was carried out to identify the functional microbial communities and their dynamics in the activated sludge at three different SRTs (25, 40 and 10 days) (Fig. 3). The identified major phyla were *Acidobacteria*, *Actinobacteria*, *Bacteroidetes*, *Chloroflexi*, *Firmicutes*, *Nitrospirae*, *Planctomycetes* and *Proteobacteria*. When the SRT was 25 or 40 days, the dominant sequence of four significant phyla was *Firmicutes* > *Proteobacteria* > *Actinobacteria* > *Bacteroidetes*, whereas with the SRT of 10 days the dominant sequence was *Proteobacteria* > *Bacteroidetes* > *Firmicutes* > *Acidobacteria* (Fig. 3a).

Firmicutes are extensively found in the environment and in activated sludge processes due to their high resistance against extreme environmental conditions (ElNaker et al., 2018). The relative abundance of *Firmicutes* in the activated sludge was ~29% of total phylum at SRT of 25 days, which decreased to 26% and 17% at SRT of 40 days and SRT of 10 days, respectively. Three major classes of *Firmicutes* were *Bacilli*, *Clostridia* and *Erysipelotrichi*, among which *Clostridia* was dominant at all the examined SRTs (Fig. 3(b)). It has been reported that, *Firmicutes* play an important role in wastewater treatment by producing a variety of enzymes that degrade a wide range of organic matter. *Proteobacteria*, which are known as butyrate, glucose, propionate and acetate utilizing bacteria (J. Liu et al., 2018), were identified as the second dominant phyla when the SRT was 25 days or 40 days and the most dominant at SRT of 10 days. Four major classes of *Proteobacteria*, namely *alpha* (α),

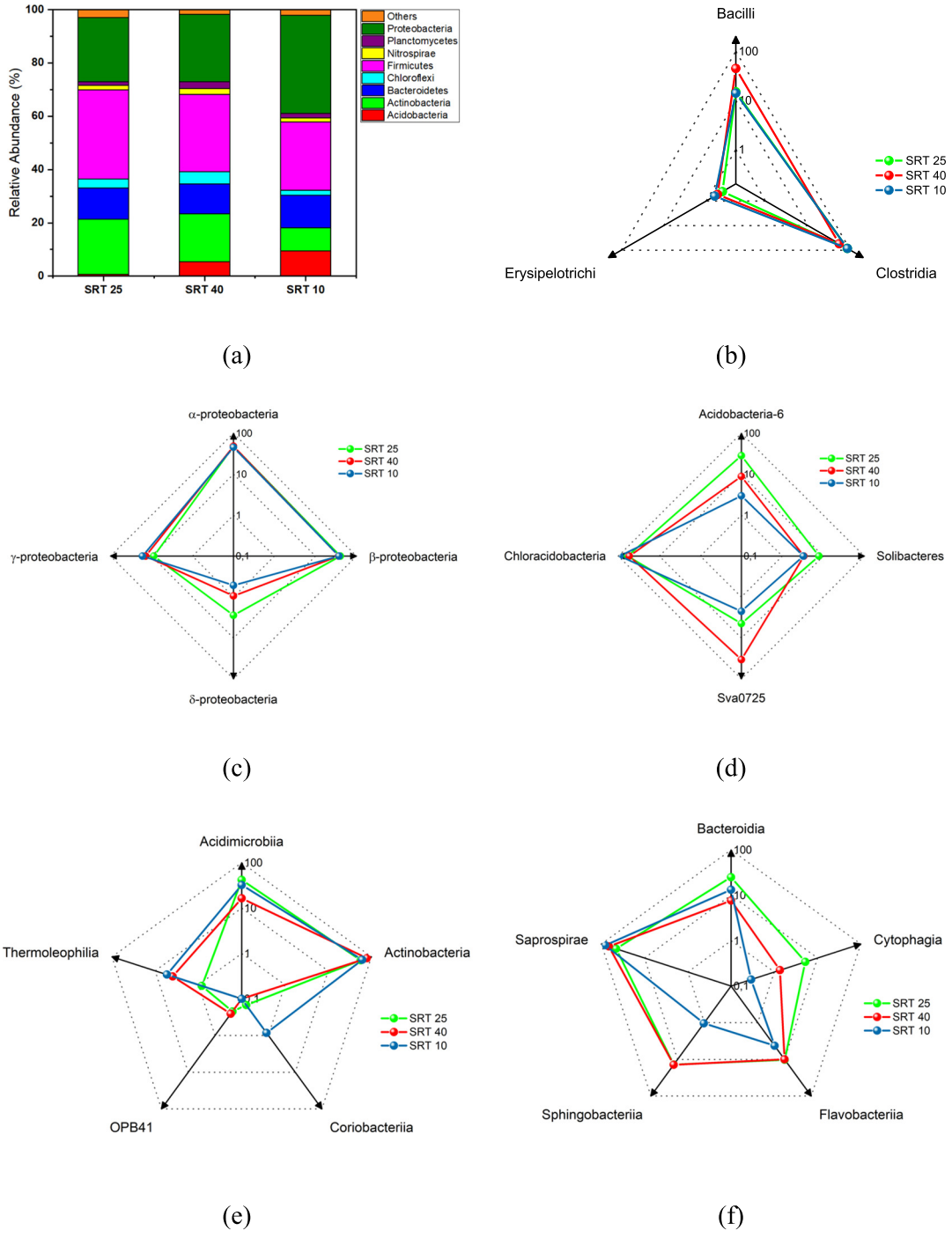

Fig. 3. (a) Relative abundance of bacterial community in phylum level at different SRTs and radar plots of major classes of phyla (b) Firmicutes, (c) Proteobacteria, (d) Acidobacteria, (e) Actinobacteria, and (f) Bacteroidetes at three different SRTs.

beta (β), *gamma* (γ) and *delta* (δ) *Proteobacteria* were identified at all SRTs. Among them, *β-Proteobacteria* and *γ-Proteobacteria* are, based on the literature, likely to be the pioneers of surface colonization on the membranes and their presence could thus lead to the drastic irretrievable membrane biofouling (Jinhua et al., 2006). The dominance of *β & γ-Proteobacteria* was observed at SRT of 10 days (Fig. 3c). Moreover, bacteria from *Firmicutes* and *Proteobacteria* phylum have been reported to produce antibiotic resistance (Zhang et al., 2019; Zhu et al., 2017).

Acidobacteria and *Actinobacteria* are capable for producing bioactive molecules by degrading complex polymeric pollutants, which are beneficial for COD reduction and microbial growth (Song et al., 2018). The relative abundance of *Acidobacteria* was at its maximum at SRT of 10 days. Among the four different classes of *Acidobacteria*, as shown in Fig. 3d, *Chloracidobacteria* was dominant at all the tested SRTs. Compared with *Acidobacteria*, *Actinobacteria* did not show any significant correlation with the SRT values. The relative abundance of *Actinobacteria* was at its maximum at SRT of 25 days and then a further decline was observed at SRT of 40 days and SRT of 10 days. Fig. 3e represents the distribution of five different classes of *Actinobacteria* at different SRTs; of which, *Acidimicrobiia* and *Actinobacteria* were predominant classes at SRT values of 25 and 40 days, respectively.

The relative abundance of *Bacteroidetes* was at its maximum at SRT of 10 days, when it accounted for 21% of the total microbial community. It has been reported that *Bacteroidetes* are responsible for the excessive release of proteinaceous EPS, which can proceed colonization and membrane fouling (Gao et al., 2010). Among the identified five different classes of *Bacteroidetes*, *Saprospirae* was the leading class at all SRTs. *Chloroflexi*, which is known as a filamentous type of bacteria, was found as 4%, 5% and 3% at SRT of 25, 40 and 10 days, respectively. This type of microorganisms are known to be responsible for bulking and foaming problems in the activated sludge (Yu et al., 2018). Apart from that, *Chloroflexi* degrades the organic matter generated from metabolic activities and lysis of dead cells (Kindaichi et al., 2012).

To analyze the microbial diversity and dynamics more thoroughly and closely, taxonomic analysis was carried out at the genus level. Heatmap in Fig. 4, represents the distribution of the top 30 microbial communities at the genus level at the different SRTs used in the experiments. *Proteiniclasticum* and *Clostridium*, which belong to *Firmicutes* phylum, were identified as the top dominant genera at SRT of 25 days, which accounts for 11% and 10% of total genera, respectively. On the other hand, at SRT of 40 days an unknown genus of the *Comamonadaceae* family, which belongs to *Proteobacteria* phylum, was the top-most genus accounted for the 7% of total genera. Similarly, at SRT of 10 days three unknown genera of three different families, *Chitinophagaceae*, *Ellin6075* and *Comamonadaceae*, which belongs to *Bacteroidetes*, *Acidobacteria* and *Proteobacteria* phylum, respectively, were the top dominant genera accounting for 9%, 9% and 8%, respectively.

Fig. 5 represents the top five genera of floc forming bacteria and quorum quenching (QQ) bacteria and their dynamics under varying solid retention times. *Paracoccus*, *TM7*, *Zoogloea*, *Flavobacterium* and *Thauera* are known as granular floc forming bacteria in the activated sludge (Zhang et al., 2016; Zhao et al., 2013). It can be seen from Fig. 5(a), that relatively high numbers of OTUs of *Paracoccus*, *TM7* and *Flavobacterium* species were observed at SRT of 25 days compared to SRTs of 40 and 10 days. Several QQ bacteria were also identified in the activated sludge, among which the top five genera were *Flavobacterium*,

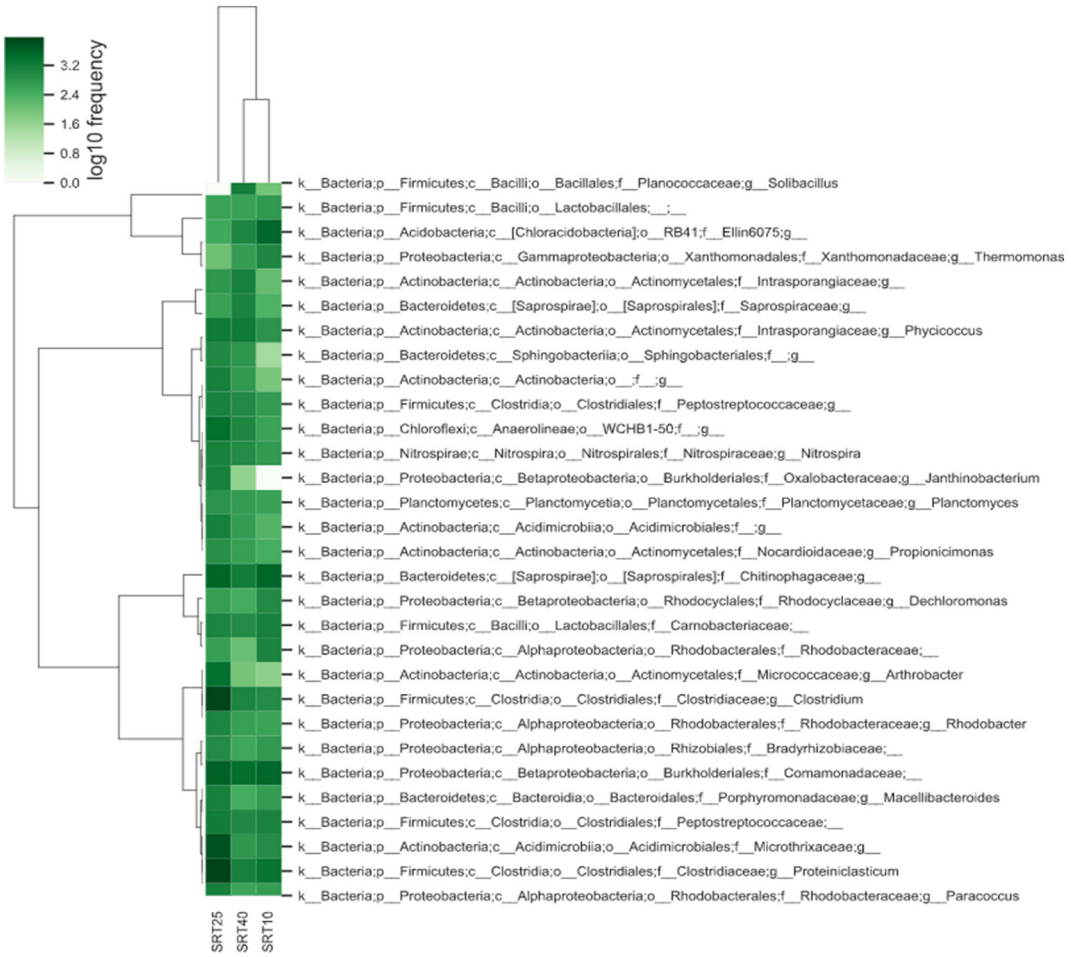

Fig. 4. Heatmap with dendrogram showing the abundance of top 30 genera in sample groups at different SRT.

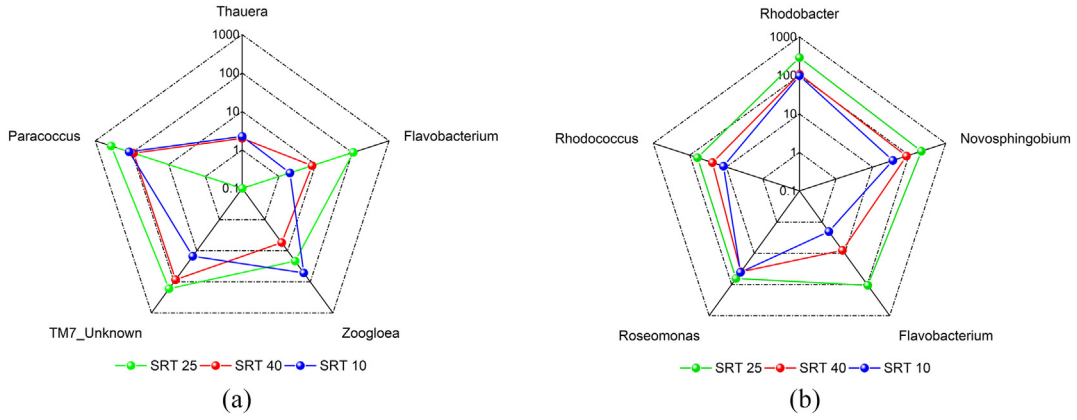

Fig. 5. Dynamics of (a) floc forming microbes and (b) QQ microbes at genus level under varying SRTs.

Novosphingobium, *Rhodobacter*, *Rhodococcus* and *Roseomonas* (Fig. 5b). These types of bacteria are prominent in reducing membrane biofouling by blocking quorum sensing (QS) signals, which are mainly responsible for bacterial communication and EPS production (Lee et al., 2018; Oh and Lee, 2018). As can be seen in Fig. 5(b), all these five bacterial genera were dominant at SRT of 25 days and further gradually decreased at SRTs of 40 and 10 days. *Nitrospira* from *Nitrospirae* phylum is well known for nitrite-oxidizing bacteria and their abundances were 2%, 2% and 1% at SRT of 25, 40 and 10 days, respectively. These results indicate that longer SRT is advantageous for the growth of denitrifying bacteria. Similar results have been reported by Yu et al. (2018).

3.2. Effect of SRT on activated sludge characteristics

3.2.1. Mixed liquor concentration and SVI

MLSS, MLVSS and SVI were monitored to determine the impact of changing SRTs on activated sludge characteristics, as shown in Fig. 6. The dashed line on each SRT phase indicates the end of the adaptation period and the beginning of a steady period. An increasing trend in the concentration of MLSS and MLVSS at longer SRT can be noted in Fig. 6.

At SRT 25, 40 and 10 the mean concentration MLSS was 6.1 ± 0.4, 10.3 ± 1.2 and 5.1 ± 0.4 g/l, respectively and the mean concentration MLVSS was 4.2 ± 0.2, 5.4 ± 0.8 and 2.9 ± 0.4 g/l, respectively. However, the ratio of MLVSS to MLSS was 0.67, 0.53 and 0.57 for SRT 25, 40 and 10, respectively. A higher ratio of MLVSS to MLSS at SRT of 25 days is attributed to the higher concentration of organic substances in the mixed liquor. In contrast, the lower ratio of MLVSS to MLSS at SRT of 40 days indicates the abundance of inert or inorganic material at higher SRT. Sludge volume index (SVI), which is an indicator of activated sludge settling characteristics (Van den Broeck et al., 2012), indicated a rather stable value during SRT of 25 days (106.6 ± 10.9 ml/g) and SRT of 40 days (94.3 ± 9.2 ml/g), while an elevated SVI was observed at SRT of 10 days (120.4 ± 27.3 ml/g). The increasing trend of SVI values with decreasing SRT indicates an exacerbated bio-flocculation state and deterioration of sludge filterability (Van den Broeck et al., 2012).

3.2.2. Concentration of EPS fractions

The production of EPS is firmly associated with the available microbial community and their activities, such as microbial growth, secretion and substrate consumption, which shows a strong correlation with the SRT (Ahmed et al., 2007; Shi et al., 2017; Yu et al., 2018). The EPS fractions (SMP, LB-EPS and TB-EPS) produced at different SRTs were characterized by their carbohydrate and protein contents, as presented in Fig. 7.

SMP is considered as the inventory of soluble organic compounds released into the mixed liquor from the metabolism of the substrate (usually with the growth of microbes) and microbial decay (Jarusutthirak and Amy, 2006). Therefore, the rate of SMP production is proportional to the microbial concentration and substrate utilization; in other words, food to microorganism ratio (F/M ratio). In this study, while dealing with real municipal wastewater, the highest concentration of

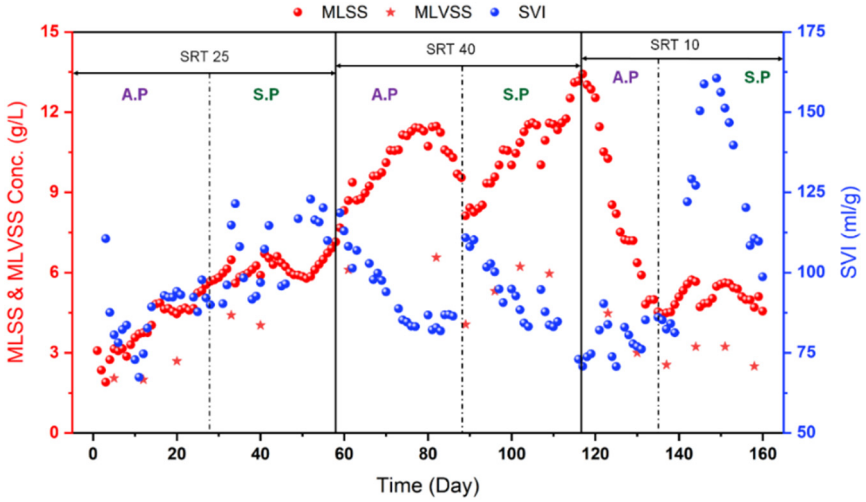

Fig. 6. Variation of MLSS, MLVSS and SVI at different SRTs. *A.P.* and *S.P.* represents the adaptation and stabilized period, respectively.

SMP was observed when the SRT was 40 days, and the lowest concentration was observed when the SRT was 25 days, as shown in Fig. 7 (a). The highest production of SMP at SRT of 40 days can be attributed to the maximum substrate concentration (1030.0 ± 223.3 mg/l) at that SRT compared to the substrate concentrations at SRT of 25 and 10 days (687.5 ± 130.7 and 795.0 ± 75.0 mg/l, respectively). Also, the longer SRT facilitates the maximum growth of biomass concentration in the bioreactor. As a result, a higher F/M ratio was observed at SRT 40 (0.38 g COD/g MLVSS·day) compared to SRT of 25 (0.29 g COD/g MLVSS·day) and 10 (0.35 g COD/g MLVSS·d) days which resulted in the highest possible microbial activity and maximum production of SMP. In a recent study on the effect of organic matter in wastewater on SMP production, Ferrer-Polonio et al. (2018) concluded that higher ratios of F/M resulted in higher concentrations of SMP. The Fig. 7 (a) also indicates that the protein fraction was dominant at SRT of 40 and 10 days in the SMP, while the carbohydrate fraction was predominant at SRT of 25 days.

LB-EPS is a highly hydrated part of the B-EPS matrix and diffuses in the outer layer. The higher correlation of LB-EPS with membrane fouling propensities has been reported due to its direct contact with membrane surface (Shi et al., 2017; Wang et al., 2009). Compared to SMP and TB-EPS, the concentrations of LB-EPS were relatively low as shown in Fig. 7 (b). At all the tested SRTs, the protein fraction of the LB-EPS was the major element over carbohydrate fraction. Similarly, the protein and carbohydrate concentrations in TB-EPS are presented in Fig. 7 (c), which indicates the higher concentration of TB-EPS observed at SRT of 10 days. Like in LB-EPS, the protein was dominant over the carbohydrate content in TB-EPS. However, 10 days of SRT were found with a higher concentration of proteins in TB-EPS while 25 days of SRT had higher carbohydrate content.

3.2.3. Floc size distribution of sludge

The floc size distribution of activated sludge in the MBR process at SRT values of 25, 40 and 10 days are presented in Fig. 7 (d). The size distributions d (0.1), d (0.5) and d (0.9) indicate 10%, 50% and 90% of the volume distribution below these values, respectively. The volume mean diameter, i.e., d (0.5) at SRT of 25, 40 and 10 days were observed as 29.0 ± 0.9, 25.3 ± 0.7 and 19.5 ± 0.5 μm, respectively. The results in Fig. 7 (d), indicate that the larger floc formation tendency was mostly seen when the SRT was 25 days, which is in consistent with the abundance of granular floc forming microbial genera analyzed at SRT of 25 days.

To understand the correlation between the SRT, the activated sludge characteristics and floc size, a statistical analysis was performed with the significance of 95% confidence level. Scattered matrix and the Pearson correlation coefficients (R) (Fig. 8) showed that d 50 floc size was strongly correlated with the SRT ($R = 0.63$). Besides that, the carbohydrate content of SMP and TB-EPS also showed a strong positive correlation with the floc size ($R = 0.82$ and 0.63, respectively). This correlation is in agreement with the results reported in other studies, where it has been stated that carbohydrate content in EPS matrix is responsible for cell aggregation and floc formation due to their high molecular weight, long carbon backbone with active side chain and gel-forming properties (Lin et al., 2014; Shi et al., 2017; Wang et al., 2009). However, a strong negative correlation was observed between the carbohydrate content of LB-EPS (LB-EPS_C) with d50 floc size,

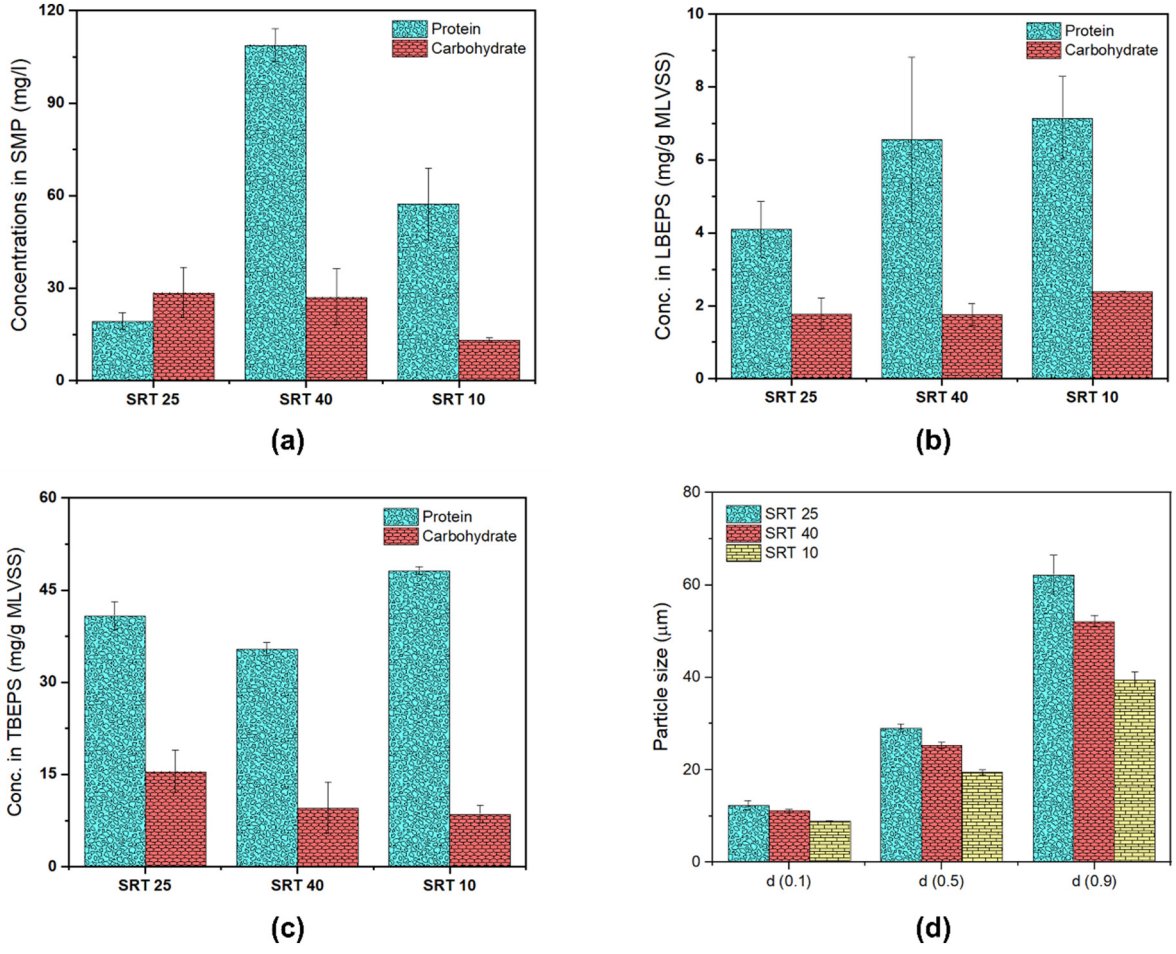

Fig. 7. Protein and carbohydrate concentration in (a) SMP, (b) LBEPS and (c) TBEPS at different SRTs and (d) floc size distribution of sludge suspension at different SRTs.

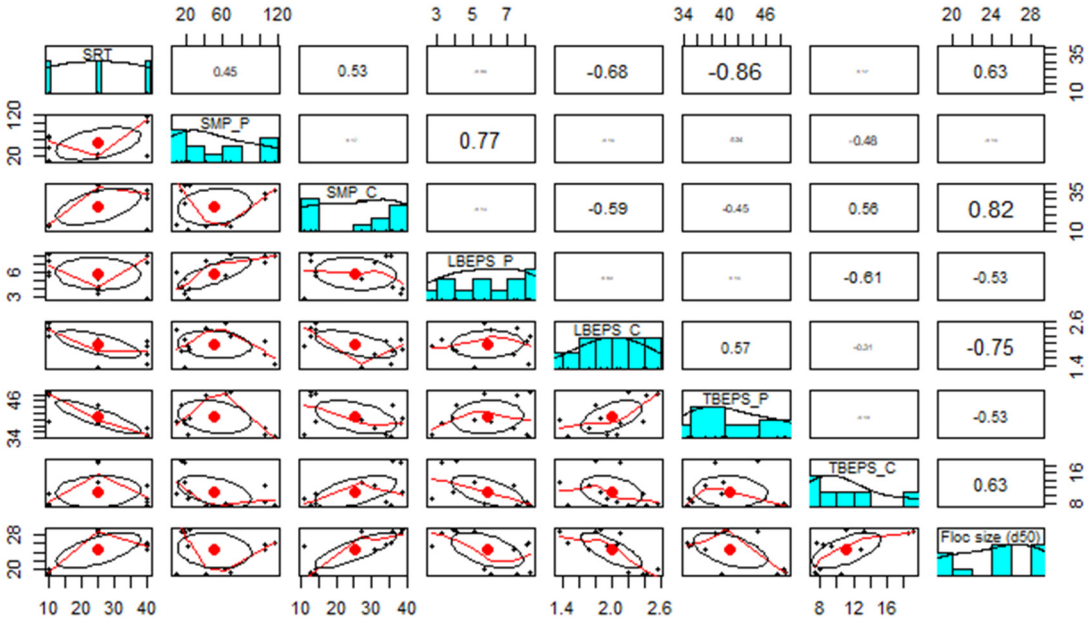

Fig. 8. Scattered Matrix and the Pearson correlation analysis of SRT, protein content of SMP (SMP_P), carbohydrate content of SMP (SMP_C), protein content of LB-EPS (LB-EPS_P), carbohydrate content of LB-EPS (LB-EPS_C), protein content of TB-EPS (TB-EPS_P), carbohydrate content of TB-EPS (TB-EPS_C) and d50 floc sizes.

which indicates the adverse effect of LB-EPS_C on the floc formation. Similarly, the protein content of the EPS fractions always showed a negative correlation ($R = -0.53$) with floc formation.

3.3. Effect of SRT on effluent quality

The MBR was operated for treating the real municipal wastewater generated from the city of Mikkeli (about 50,000 inhabitants), a Southern Savonia region of the Eastern Finland. Therefore, a dynamic influent characteristic was observed over the operational period. The results of influent wastewater and permeate characteristics are listed in Table 1.

The highest concentrations of water quality indicators, such as BOD, COD, TP, TN and NH_4-N, were observed in the influent during the operational period of the SRT of 40 days. The corresponding removal efficiencies of the water quality indicators are illustrated in Fig. 9. Despite of operating the MBR at different SRTs, an excellent permeate quality was obtained over the whole experimental period (Table 1). COD removal rate was at its maximum (97.0 ± 1.2%) at SRT of 40 days despite of having maximum influent COD concentration. The maximum removal of COD at SRT of 40 days can be attributed to the higher biomass concentration, which facilitates the decomposition of various organic compounds. The removal rate of TP and NH_4-N were more than 98.5% over the whole experimental period, although the SRT value was changed occasionally. However, total nitrogen removal was relatively low as compared to other indicators (Table 1), demonstrating a poor anoxic condition that needs to be optimized further according to the need of discharge limits. The maximum removal of the TN was observed at SRT of 40 days (70.3%), while it was at its minimum at SRT of 25 days (56.6%).

3.4. Effect of SRT on membrane fouling

The TMP profile (Fig. 10) was monitored over the operational period at different SRT with a permeate flux of 15 L/(h·m^2). From the TMP profile, it can be visualized that the longest operational period (26 days) of MBR prior to TMP rise to the value of 50 mbar was observed at SRT 25. Whereas the TMP reaches at 50 mbar within 21 days and 12 days of operation at SRT 40 and 10, respectively.

The TMP profiles during MBR operation can be distinguished as four different stages, including a sharp TMP rise, flux stabilization followed by a slow and fast TMP rise. At all the tested SRTs, after the membrane cleaning events, a rapid rise of TMP occurred within a day of operation, followed by well stabilized TMP profile (from the first datapoint to the second datapoint in Fig. 10), which may be due to the rapid growth of biofilm on the membrane surface (Pronk et al., 2019). This stabilized stage was 3 days long when the SRT was 25 and 10 days, while it was 11 days long when the SRT was 40 days. The prolonged stable operation at SRT of 40 days can be attributed to the adequate abrasion effect of high MLSS concentration that prevented the rapid growth of biofilm on the membrane surface (Meng et al., 2006). The slow TMP rising stages continued 14, 8 and 4 days at the SRTs of 25, 40 and 10 days, with an approximate rate of TMP rise 1.32, 1.53 and 2.52 mbar/day,

Table 1
Characteristics of influent wastewater and permeate at different SRTs (for SRT 25 and 40, number of samples = 4 and for SRT 10 no of samples = 3).

Water quality parameters	SRT 25 days		SRT 40 days		SRT 10 days	
	Influent	Permeate	Influent	Permeate	Influent	Permeate
Temperature, °C	13.8 ± 1.6	16.1 ± 0.8	16.6 ± 0.5	19.2 ± 0.4	15.4 ± 0.9	18.7 ± 0.3
pH	7.2 ± 0.1	6.9 ± 0.2	7.3 ± 0.0	6.7 ± 0.1	7.2 ± 0.1	6.7 ± 0.2
BOD, mg/l	305.0 ± 71.6	2.9 ± 0.2	362.5 ± 84.1	3.0 ± 0.0	360.0 ± 40.0	3.3 ± 0.5
COD, mg/l	687.5 ± 130.7	26.5 ± 6.4	1030.0 ± 223.3	28.3 ± 5.9	795.0 ± 75.0	33.3 ± 4.7
TP, mg/l	8.9 ± 1.8	0.1 ± 0.0	11.1 ± 1.4	0.2 ± 0.0	11.0 ± 1.0	0.2 ± 0.1
TN, mg/l	56.5 ± 7.4	24.8 ± 1.9	77.3 ± 6.9	25.8 ± 2.3	74.5 ± 0.5	24.0 ± 2.4
NH_4-N, mg/l	41.8 ± 3.6	0.6 ± 0.9	59.0 ± 9.4	0.1 ± 0.0	56.5 ± 2.5	0.1 ± 0.0

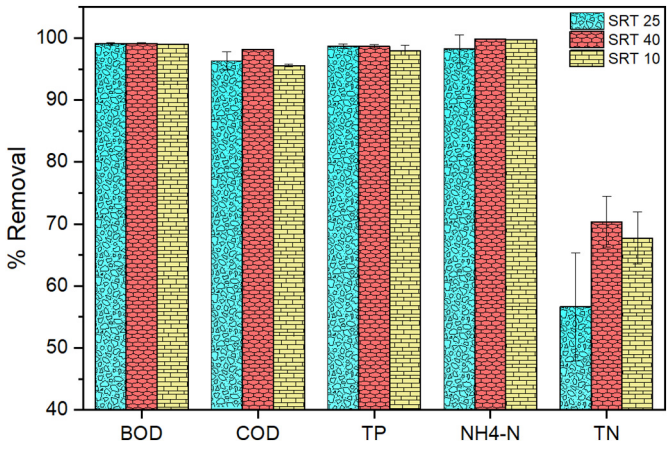

Fig. 9. Removal efficiencies of tested water quality indicators at different SRTs.

respectively. In the final stage, the TMP jump stage, the rate of TMP rise was 2.22, 15.38 and 10.04 mbar/day for SRT of 25, 40 and 10 days, respectively. Therefore, it can be concluded from these experiments that the process operation with the SRT value of 25 days led to the possibility of operating a long time with a steady rise of TMP.

The TMP profile at different SRTs can also be explained from the results obtained from the microbial community analysis, sludge characteristics and floc size distribution analysis during the MBR operation. When SRT was 25 days, higher number of OTUs of QQ-bacteria and floc forming bacteria were observed (Fig. 5), which favors the lower membrane fouling and larger floc formation, respectively. Apart from that, the lowest values for the EPS excretion were seen at SRT of 25 days (Fig. 7). On the other hand, the highest EPS concentration was observed at SRT of 40 days. However, high MLSS concentration (Fig. 6) and large floc formation (Fig. 7 (d)) at SRT of 40 days might have promoted the better membrane scouring and lower filtration resistance, which may prolong the operational period under the TMP of 50 mbar of MBR as compared to SRT of 10 days (Shen et al., 2015; Zhang and Jiang, 2019). The rapid membrane fouling observed at the SRT of 10 days was a result from the microbial community, floc size and EPS concentration. The particle size analysis showed the poor floc formation at SRT value of 10 days, which may have resulted from the abundance of solutes and colloids in the bulk sludge suspension. Sub-micron size of sludge flocs and solutes can readily be deposited on to the membrane surface due to suction drag force, leading to severe membrane fouling (Guo et al., 2012).

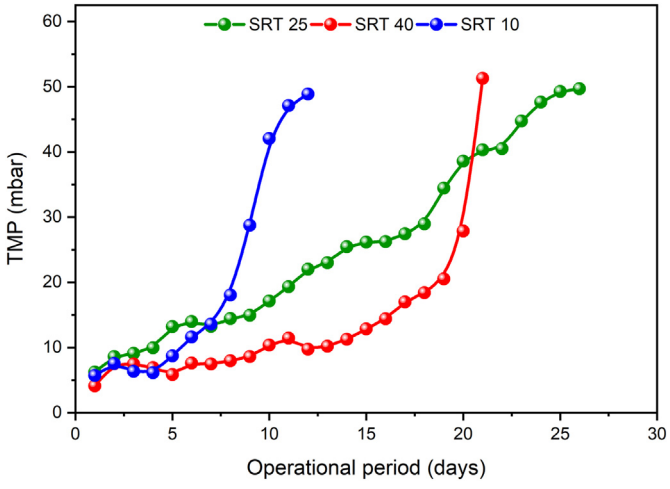

Fig. 10. TMP profiles obtained at different SRTs with an operating flux of 15 L/(h·m^2). TMP was monitored online, and data were recorded for every 10 s. Each day data was the average of the 8640 data point.

4. Conclusion

The outcome of this research in a pilot-scale gravity-driven A/O MBR system demonstrates that SRT has a substantial effect on microbial community dynamics, activated sludge characteristics, floc size distribution and membrane fouling. Results obtained from the microbial community analysis revealed that SRT of 25 days was in this case superior with microbial species richness, while SRT of 40 days was a high diverse collection of the microbial species. The production of SMP was minimum at SRT of 25 days, which was also dependent on the F/M ratio. The carbohydrate content of the SMP and TB-EPS fraction was maximum at SRT of 25 days, which was found to be responsible for the largest floc formation. The most extended operational period and the lowest rate of membrane fouling was observed at SRT of 25 which was resulted from the superior microbial community, lowest production of SMP and LB-EPS as well as the lower filtration resistance of larger sludge flocs. Relative abundance of QQ bacteria and granular floc forming bacterial genera at SRT 25 provided less membrane fouling tendency and larger floc formation, respectively. On the other hand, abundance of various surface colonizing and EPS producing bacteria was found at SRT 10, which promoted the membrane fouling at that SRT. Therefore, according to this study it can be concluded that, an optimized SRT will prevent rapid membrane fouling in large-scale GD-MBR applications by regulating the microbial community dynamics and resulting biochemical properties of the mixed liquor and microbial flocs.

CRediT authorship contribution statement

Anjan Deb: Conceptualization, Methodology, Formal analysis, Investigation, Writing – original draft, Project administration. **Khum Gurung:** Conceptualization, Supervision, Writing – review & editing, Project administration, Funding acquisition. **Jannatul Rumky:** Methodology, Writing – review & editing. **Mika Sillanpää:** Supervision, Writing – review & editing, Project administration, Funding acquisition. **Mika Mänttäri:** Writing – review & editing, Project administration. **Mari Kallioinen:** Writing – review & editing, Supervision.

Declaration of competing interest

The authors declare that they have no known competing financial interests or personal relationships that could have appeared to influence the work reported in this paper.

Acknowledgements

The authors would like to acknowledge Regional Council of South Savo (Etelä-Savon Maakuntaliitto, Finland) under the EU (Finnish Structural Funds) Program for the financial support for this research (Decision number: EURA 2014/7154/09 02 01 01/2018/ESAVO). The authors are also thankful to Reijo Turkki, Anne Bergman, Risto Repo, Christiina Liikanen, Reetta Turkki, Päivi Luukkonen and all other staffs of Mikkeli Wastewater Treatment Plant (Mikkeli Vesilaitos) for their support during the MBR process operation and some laboratory services. Microbial community analysis support from Biocenter Oulu is also thankfully acknowledged.

References

Ahmed, Z., Cho, J., Lim, B.-R., Song, K.-G., Ahn, K.-H., 2007. Effects of sludge retention time on membrane fouling and microbial community structure in a membrane bioreactor. J. Membr. Sci. 287, 211–218. https://doi.org/10.1016/j.memsci.2006.10.036.

Bokulich, N.A., Kaehler, B.D., Rideout, J.R., Dillon, M., Bolyen, E., Knight, R., Huttley, G.A., Gregory Caporaso, J., 2018. Optimizing taxonomic classification of marker-gene

amplicon sequences with QIIME 2's q2-feature-classifier plugin. Microbiome 6, 90. https://doi.org/10.1186/s40168-018-0470-z.

Callahan, B.J., McMurdie, P.J., Rosen, M.J., Han, A.W., Johnson, A.J.A., Holmes, S.P., 2016. DADA2: high-resolution sample inference from illumina amplicon data. Nat. Methods 13, 581–583. https://doi.org/10.1038/nmeth.3869.

Caporaso, J.G., Kuczynski, J., Stombaugh, J., Bittinger, K., Bushman, F.D., Costello, E.K., Fierer, N., Peña, A.G., Goodrich, J.K., Gordon, J.I., Huttley, G.A., Kelley, S.T., Knights, D., Koenig, J.E., Ley, R.E., Lozupone, C.A., McDonald, D., Muegge, B.D., Pirrung, M., Reeder, J., Sevinsky, J.R., Turnbaugh, P.J., Walters, W.A., Widmann, J., Yatsunenko, T., Zaneveld, J., Knight, R., 2010. QIIME allows analysis of high-throughput community sequencing data. Nat. Methods 7, 335–336. https://doi.org/10.1038/nmeth.f.303.

Chen, M., Zhang, X., Wang, Z., Wang, L., Wu, Z., 2017. QAC modified PVDF membranes: antibiofouling performance, mechanisms, and effects on microbial communities in an MBR treating municipal wastewater. Water Res. 120, 256–264. https://doi.org/10.1016/j.watres.2017.05.012.

Clesceri, L.S., Greenberg, A.E., Eaton, A.D., 1998. Standard Methods for the Examination of Water and Wastewater. American Public Health Association, Washington, DC, pp. 4–415.

Deng, L., Guo, W., Ngo, H.H., Zuthi, M.F.R., Zhang, J., Liang, S., Li, J., Wang, J., Zhang, X., 2015. Membrane fouling reduction and improvement of sludge characteristics by bioflocculant addition in submerged membrane bioreactor. Sep. Purif. Technol. 156, 450–458. https://doi.org/10.1016/j.seppur.2015.10.034.

Duan, L., Song, Y., Yu, H., Xia, S., Hermanowicz, S.W., 2014. The effect of solids retention times on the characterization of extracellular polymeric substances and soluble microbial products in a submerged membrane bioreactor. Bioresour. Technol. 163, 395–398. https://doi.org/10.1016/j.biortech.2014.04.112.

ElNaker, N.A., Elektorowicz, M., Naddeo, V., Hasan, S.W., Yousef, A.F., 2018. Assessment of microbial community structure and function in serially passaged wastewater electrobioreactor sludge: an approach to enhance sludge settleability. Sci. Rep. 8, 7013. https://doi.org/10.1038/s41598-018-25509-2.

Ferrer-Polonio, E., Fernández-Navarro, J., Alonso-Molina, J.L., Bes-Piá, A., Mendoza-Roca, J.A., 2018. Influence of organic matter type in wastewater on soluble microbial products production and on further ultrafiltration. J. Chem. Technol. Biotechnol. 93, 3284–3291. https://doi.org/10.1002/jctb.5689.

Fortunato, L., Ranieri, L., Naddeo, V., Leiknes, T., 2020. Fouling control in a gravity-driven membrane (GDM) bioreactor treating primary wastewater by using relaxation and/or air scouring. J. Membr. Sci. 610, 118261. https://doi.org/10.1016/j.memsci.2020.118261.

Frølund, B., Palmgren, R., Keiding, K., Nielsen, P.H., 1996. Extraction of extracellular polymers from activated sludge using a cation exchange resin. Water Res. 30, 1749–1758. https://doi.org/10.1016/0043-1354(95)00323-1.

Gao, D.-W., Zhang, T., Tang, C.-Y.Y., Wu, W.-M., Wong, C.-Y., Lee, Y.H., Yeh, D.H., Criddle, C.S., 2010. Membrane fouling in an anaerobic membrane bioreactor: differences in relative abundance of bacterial species in the membrane foulant layer and in suspension. J. Membr. Sci. 364, 331–338. https://doi.org/10.1016/j.memsci.2010.08.031.

Guo, W., Ngo, H.-H., Li, J., 2012. A mini-review on membrane fouling. Bioresour. Technol. 122, 27–34. https://doi.org/10.1016/j.biortech.2012.04.089.

Gurung, K., Ncibi, M.C., Sillanpää, M., 2017. Assessing membrane fouling and the performance of pilot-scale membrane bioreactor (MBR) to treat real municipal wastewater during winter season in nordic regions. Sci. Total Environ. https://doi.org/10.1016/j.scitotenv.2016.11.122.

Gurung, K., Ncibi, M.C., Sillanpää, M., 2019. Removal and fate of emerging organic micropollutants (EOMs) in municipal wastewater by a pilot-scale membrane bioreactor (MBR) treatment under varying solid retention times. Sci. Total Environ. 667, 671–680. https://doi.org/10.1016/j.scitotenv.2019.02.308.

Han, S.-S., Bae, T.-H., Jang, G.-G., Tak, T.-M., 2005. Influence of sludge retention time on membrane fouling and bioactivities in membrane bioreactor system. Process Biochem. 40, 2393–2400. https://doi.org/10.1016/j.procbio.2004.09.017.

Jarusutthirak, C., Amy, G., 2006. Role of soluble microbial products (SMP) in membrane fouling and flux decline. Environ. Sci. Technol. 40, 969–974. https://doi.org/10.1021/es050987a.

Jinhua, P., Fukushi, K., Yamamoto, K., 2006. Bacterial community structure on membrane surface and characteristics of strains isolated from membrane surface in submerged membrane bioreactor. Sep. Sci. Technol. 41, 1527–1549. https://doi.org/10.1080/01496390600683571.

Katoh, K., Standley, D.M., 2013. MAFFT multiple sequence alignment software version 7: improvements in performance and usability. Mol. Biol. Evol. 30, 772–780. https://doi.org/10.1093/molbev/mst010.

Kindaichi, T., Yuri, S., Ozaki, N., Ohashi, A., 2012. Ecophysiological role and function of uncultured chloroflexi in an anammox reactor. Water Sci. Technol. 66, 2556–2561. https://doi.org/10.2166/wst.2012.479.

Krzeminski, P., Leverette, L., Malamis, S., Katsou, E., 2017. Membrane bioreactors – a review on recent developments in energy reduction, fouling control, novel con fi gurations, LCA and market prospects. J. Membr. Sci. 527, 207–227. https://doi.org/10.1016/j.memsci.2016.12.010.

Laera, G., Giordano, C., Pollice, A., Saturno, D., Mininni, G., 2007. Membrane bioreactor sludge rheology at different solid retention times. Water Res. 41, 4197–4203. https://doi.org/10.1016/j.watres.2007.05.032.

Lee, W., Kang, S., Shin, H., 2003. Sludge characteristics and their contribution to microfiltration in submerged membrane bioreactors. J. Membr. Sci. 216, 217–227. https://doi.org/10.1016/S0376-7388(03)00073-5.

Lee, K., Yu, H., Zhang, X., Choo, K.-H., 2018. Quorum sensing and quenching in membrane bioreactors: opportunities and challenges for biofouling control. Bioresour. Technol. 270, 656–668. https://doi.org/10.1016/j.biortech.2018.09.019.

Li, X.Y., Yang, S.F., 2007. Influence of loosely bound extracellular polymeric substances (EPS) on the flocculation, sedimentation and dewaterability of activated sludge. Water Res. 41, 1022–1030. https://doi.org/10.1016/j.watres.2006.06.037.

Li, X.-F., Li, Y.-J., Liu, H., Hua, Z.-Z., Du, G.-C., Chen, J., 2008. Correlation between extracellular polymeric substances and aerobic biogranulation in membrane bioreactor. Sep. Purif. Technol. 59, 26–33. https://doi.org/10.1016/j.seppur.2007.05.024.

Lin, H., Zhang, M., Wang, F., Meng, F., Liao, B.-Q., Hong, H., Chen, J., Gao, W., 2014. A critical review of extracellular polymeric substances (EPSs) in membrane bioreactors: characteristics, roles in membrane fouling and control strategies. J. Membr. Sci. 460, 110–125. https://doi.org/10.1016/j.memsci.2014.02.034.

Liu, J., Tian, Z., Zhang, P., Qiu, G., Wu, Y., Zhang, H., Xu, R., Fang, W., Ye, J., Song, Y., Zeng, G., 2018. Influence of reflux ratio on two-stage anoxic/oxic with MBR for leachate treatment: performance and microbial community structure. Bioresour. Technol. 256, 69–76. https://doi.org/10.1016/j.biortech.2018.01.146.

Liu, Y., Liu, Q., Li, J., Ngo, H.H., Guo, W., Hu, J., Gao, M., Wang, Q., Hou, Y., 2018. Effect of magnetic powder on membrane fouling mitigation and microbial community/composition in membrane bioreactors (MBRs) for municipal wastewater treatment. Bioresour. Technol. 249, 377–385. https://doi.org/10.1016/j.biortech.2017.10.027.

Long, Y., Yu, G., Dong, L., Xu, Y., Lin, H., Deng, Y., You, X., Yang, L., Liao, B.-Q., 2021. Synergistic fouling behaviors and mechanisms of calcium ions and polyaluminum chloride associated with alginate solution in coagulation-ultrafiltration (UF) process. Water Res. 189, 116665. https://doi.org/10.1016/j.watres.2020.116665.

McDonald, D., Price, M.N., Goodrich, J., Nawrocki, E.P., DeSantis, T.Z., Probst, A., Andersen, G.L., Knight, R., Hugenholtz, P., 2012. An improved greengenes taxonomy with explicit ranks for ecological and evolutionary analyses of bacteria and archaea. ISME J. 6, 610–618. https://doi.org/10.1038/ismej.2011.139.

Meng, F., Zhang, H., Yang, F., Zhang, S., Li, Y., Zhang, X., 2006. Identification of activated sludge properties affecting membrane fouling in submerged membrane bioreactors. Sep. Purif. Technol. 51, 95–103. https://doi.org/10.1016/j.seppur.2006.01.002.

Meng, F., Yang, F., Shi, B., Zhang, H., 2008. A comprehensive study on membrane fouling in submerged membrane bioreactors operated under different aeration intensities. Sep. Purif. Technol. 59, 91–100. https://doi.org/10.1016/j.seppur.2007.05.040.

Meng, F., Zhang, S., Oh, Y., Zhou, Z., 2017. Fouling in membrane bioreactors : an updated review. Water Res. 114, 151–180. https://doi.org/10.1016/j.watres.2017.02.006.

Oh, H.-S., Lee, C.-H., 2018. Origin and evolution of quorum quenching technology for biofouling control in MBRs for wastewater treatment. J. Membr. Sci. 554, 331–345. https://doi.org/10.1016/j.memsci.2018.03.019.

Ouyang, K., Liu, J., 2009. Effect of sludge retention time on sludge characteristics and membrane fouling of membrane bioreactor. J. Environ. Sci. 21, 1329–1335. https://doi.org/10.1016/S1001-0742(08)62422-5.

Price, M.N., Dehal, P.S., Arkin, A.P., 2010. FastTree 2 – approximately maximum-likelihood trees for large alignments. PLoS One 5, e9490. https://doi.org/10.1371/journal.pone.0009490.

Pronk, W., Ding, A., Morgenroth, E., Derlon, N., Desmond, P., Burkhardt, M., Wu, B., Fane, A.G., 2019. Gravity-driven membrane filtration for water and wastewater treatment: a review. Water Res. 149, 553–565. https://doi.org/10.1016/j.watres.2018.11.062.

Raunkjær, K., Hvitved-Jacobsen, T., Nielsen, P.H., 1994. Measurement of pools of protein, carbohydrate and lipid in domestic wastewater. Water Res. 28, 251–262. https://doi.org/10.1016/0043-1354(94)90261-5.

Rumky, J., Ncibi, M.C., Burgos-Castillo, R.C., Deb, A., Sillanpää, M., 2018. Optimization of integrated ultrasonic-Fenton system for metal removal and dewatering of anaerobically digested sludge by box-behnken design. Sci. Total Environ. 645, 573–584. https://doi.org/10.1016/j.scitotenv.2018.07.125.

Shen, L., Lei, Q., Chen, J.-R., Hong, H.-C., He, Y.-M., Lin, H.-J., 2015. Membrane fouling in a submerged membrane bioreactor: impacts of floc size. Chem. Eng. J. 269, 328–334. https://doi.org/10.1016/j.cej.2015.02.002.

Shi, Y., Huang, J., Zeng, G., Gu, Y., Chen, Y., Hu, Y., Tang, B., Zhou, J., Yang, Y., Shi, L., 2017. Exploiting extracellular polymeric substances (EPS) controlling strategies for performance enhancement of biological wastewater treatments: an overview. Chemosphere 180, 396–411. https://doi.org/10.1016/j.chemosphere.2017.04.042.

Song, D., Zhang, W., Liu, C., Wang, P., Sun, Z., Zhao, L., Zhai, X., Qi, J., Ma, J., 2018. Development of a novel anoxic/oxic fed-batch membrane bioreactor (AFMBR) based on gravity-driven and partial aeration modes: a pilot scale study. Bioresour. Technol. 270, 255–262. https://doi.org/10.1016/j.biortech.2018.08.049.

Su, X., Li, S., Xie, M., Tao, L., Zhou, Y., Xiao, Y., Lin, H., Chen, J., Sun, F., 2021. Enhancement of polychlorinated biphenyl biodegradation by resuscitation promoting factor (Rpf) and rpf-responsive bacterial community. Chemosphere 263, 128283. https://doi.org/10.1016/j.chemosphere.2020.128283.

Takimoto, Y., Hatamoto, M., Soga, T., Kuratate, D., Watari, T., Yamaguchi, T., 2021. Maintaining microbial diversity mitigates membrane fouling of an anoxic/oxic membrane bioreactor under starvation condition. Sci. Total Environ. 759, 143474. https://doi.org/10.1016/j.scitotenv.2020.143474.

Teng, J., Zhang, M., Leung, K.-T., Chen, J., Hong, H., Lin, H., Liao, B.-Q., 2019. A unified thermodynamic mechanism underlying fouling behaviors of soluble microbial products (SMPs) in a membrane bioreactor. Water Res. 149, 477–487. https://doi.org/10.1016/j.watres.2018.11.043.

Van den Broeck, R., Van Dierdonck, J., Nijskens, P., Dotremont, C., Krzeminski, P., van der Graaf, J.H.J.M., van Lier, J.B., Van Impe, J.F.M., Smets, I.Y., 2012. The influence of solids retention time on activated sludge bioflocculation and membrane fouling in a membrane bioreactor (MBR). J. Membr. Sci. 401–402, 48–55. https://doi.org/10.1016/j.memsci.2012.01.028.

Wang, Z., Wu, Z., Tang, S., 2009. Extracellular polymeric substances (EPS) properties and their effects on membrane fouling in a submerged membrane bioreactor. Water Res. 43, 2504–2512. https://doi.org/10.1016/j.watres.2009.02.026.

Wang, X., Chen, Y., Yuan, B., Li, X., Ren, Y., 2014. Impacts of sludge retention time on sludge characteristics and membrane fouling in a submerged osmotic membrane

bioreactor. Bioresour. Technol. 161, 340–347. https://doi.org/10.1016/j.biortech.2014.03.058.
Wu, M., Chen, Y., Lin, H., Zhao, L., Shen, L., Li, R., Xu, Y., Hong, H., He, Y., 2020. Membrane fouling caused by biological foams in a submerged membrane bioreactor: mechanism insights. Water Res. 181, 115932. https://doi.org/10.1016/j.watres.2020.115932.
Xie, M., Xu, L., Zhang, R., Zhou, Y., Xiao, Y., Su, X., Shen, C., Sun, F., Hashmi, M.Z., Lin, H., Chen, J., 2021. Viable but nonculturable state of yeast Candida sp. strain LN1 induced by high phenol concentrations. Appl. Environ. Microbiol. 87. https://doi.org/10.1128/AEM.01110-21.
Yu, L., Yang, Y., Yang, B., Li, Z., Zhang, X., Hou, Y., Lei, L., Zhang, D., 2018. Effects of solids retention time on the performance and microbial community structures in membrane bioreactors treating synthetic oil refinery wastewater. Chem. Eng. J. 344, 462–468. https://doi.org/10.1016/j.cej.2018.03.073.
Yurtsever, A., Basaran, E., Ucar, D., Sahinkaya, E., 2021. Self-forming dynamic membrane bioreactor for textile industry wastewater treatment. Sci. Total Environ. 751, 141572. https://doi.org/10.1016/j.scitotenv.2020.141572.
Zhang, W., Jiang, F., 2019. Membrane fouling in aerobic granular sludge (AGS)-membrane bioreactor (MBR): effect of AGS size. Water Res. 157, 445–453. https://doi.org/10.1016/j.watres.2018.07.069.
Zhang, Q., Hu, J., Lee, D.-J., 2016. Aerobic granular processes: current research trends. Bioresour. Technol. 210, 74–80. https://doi.org/10.1016/j.biortech.2016.01.098.
Zhang, Q.-Q., Bai, Y.-H., Wu, J., Xu, L.-Z.-J., Zhu, W.-Q., Tian, G.-M., Zheng, P., Xu, X.-Y., Jin, R.-C., 2019. Microbial community evolution and fate of antibiotic resistance genes in anammox process under oxytetracycline and sulfamethoxazole stresses. Bioresour. Technol. 293, 122096. https://doi.org/10.1016/j.biortech.2019.122096.
Zhao, Y., Huang, J., Zhao, H., Yang, H., 2013. Microbial community and N removal of aerobic granular sludge at high COD and N loading rates. Bioresour. Technol. 143, 439–446. https://doi.org/10.1016/j.biortech.2013.06.020.
Zhu, Y., Wang, Y., Jiang, X., Zhou, S., Wu, M., Pan, M., Chen, H., 2017. Microbial community compositional analysis for membrane bioreactor treating antibiotics containing wastewater. Chem. Eng. J. 325, 300–309. https://doi.org/10.1016/j.cej.2017.05.073.